

# MASTER

MECHANICAL AND PHYSICAL PROPERTIES OF  
IRRADIATED TYPE 348 STAINLESS STEEL\*

J. M. Beeston

DISCLAIMER

This book was prepared as an account of work sponsored by an agency of the United States Government. Neither the United States Government nor any agency thereof, nor any of their employees, makes any warranty, express or implied, or assumes any legal liability or responsibility for the accuracy, completeness, or usefulness of any information, apparatus, product, or process disclosed, or represents that its use would not infringe privately owned rights. Reference herein to any specific commercial product, process, or service by trade name, trademark, manufacturer, or otherwise, does not necessarily constitute or imply its endorsement, recommendation, or favoring by the United States Government or any agency thereof. The views and opinions of authors expressed herein do not necessarily state or reflect those of the United States Government or any agency thereof.

\* Work done under Department of Energy Contract

EY-76-C-07-1570

The submitted manuscript has been authored by a contractor of the U.S. Government under DOE Contract No. DE-AC07-76ID01570. Accordingly, the U.S. Government retains a nonexclusive, royalty-free license to publish or reproduce the published form of this contribution, or allow others to do so, for U.S. Government purposes.

#### **ACKNOWLEDGEMENTS**

**The release of data from the fracture toughness tests conducted at Bettis Atomic Power Laboratory is gratefully acknowledged.**

## ABSTRACT

A type 348 stainless steel in-pile tube irradiated to a fluence of  $3 \times 10^{22} \text{ n/cm}^2$ ,  $E > 1 \text{ MeV}$  (57 dpa), was destructively examined. The service had resulted in a maximum total creep of 1.8% at the high fluence. The metal temperature ranged between 623 and 652 K, hence the thermal creep portion of the total was negligible. Total creep was greater than had been anticipated from creep data for austenitic stainless steels irradiated in other reactors. The objectives of the destructive examination were to determine the service-induced changes of mechanical and physical properties, and to assess the possibility of adverse effects of both these changes and the greater total creep on the prospective service life of other tubes.

Measured bowing (0.51 mm) was correlated with a structural model. Post irradiation measurements included immersion density, fracture toughness, tensile strength and ductility, and creep-rupture strength. A reduction in fracture toughness due to irradiation creep was apparent.

**Key Words**

**Irradiated Type 348 stainless steel, irradiation  
creep, immersion density, bowing, swelling, fracture  
toughness, tensile strength, uniform elongation,  
creep-rupture strength.**

## MECHANICAL AND PHYSICAL PROPERTIES OF

### IRRADIATED TYPE 348 STAINLESS STEEL

J. M. Beeston

#### 1. INTRODUCTION

Radiation-induced deformation is of importance to reactor-core component service life. The dimensional stability of components as affected by swelling and irradiation creep has received attention<sup>[1,2,3]</sup>, however structural models for calculating the bulging and bowing are limited and the damaging effect of irradiation creep is relatively undefined. Irradiation creep of reactor components has been considered nondamaging<sup>[4]</sup>, and in-reactor rupture life after irradiation creep appears longer<sup>[5]</sup> than predicted by postirradiation tests.

The materials properties of an Advanced Test Reactor (ATR) Type 348 stainless steel in-pile tube (SN-5) irradiated to a peak fluence of  $2.8 \times 10^{22}$

$\text{n/cm}^2$  ( $E > 1\text{MeV}$ ) were measured on sections and specimens from the core region of the tube. The tube had operated at a volume average metal temperature (reactor centerline) of 623-652 K (660-713°F) from June 8, 1969 to March 26 1978. The amount of creep experienced (diametral measurements by bore gage) was larger (1.8 percent) than other tubes had shown after irradiation to higher fluences.

Irradiation creep to 1 percent  $\Delta D/D$  at irradiation temperatures of 650 to 857 K was previously shown to be nondamaging to postirradiation biaxial stress rupture life in transient burst tests.<sup>[4]</sup> The purpose of the present tests was to evaluate possible damage to the mechanical properties and integrity of the tube from the increased irradiation creep. The tests reported concern the dimensional stability as measured by straightness, bulging, and bowing of the tube, as well as determinations of immersion density, and tensile, fracture toughness, and creep-rupture.

## 2. PROCEDURE

A 1.2-m (4 ft) section was removed from the pressure tube at an elevation corresponding to the reactor core. A 0.6-m (2 ft) section was removed directly below the 1.2-m (4 ft) section, Figure 1. Rings were identified (Numbers 1, 4, 5, and 6) from which baseline and test specimens were to be machined. Other rings were reserved for future work. The percent chemical composition of the Type 384 stainless steel was: C - 0.037, Mn - 1.24, P - 0.011, Si - 0.47, S - 0.008, Cr - 18.05, Ni - 11.08, Mo - 0.03, Cu - 0.047, Cb and Ta - 0.55, Ta - 0.013, Co - 0.024.

### 2.1 Bore Gage Measurement

The in-pile tube before destructive testing was bore-gaged at 0.1-m (4 in.) intervals between the elevations of 23.5-m (77 ft) and 25.3-m (83 ft) [i.e. from 0.3-m (1 ft)] below the bottom of the active core to 0.3-m (1 ft) above. The results of these measurements (Figure 2) showed that the inside diameter (D) of the tube gradually increased to a

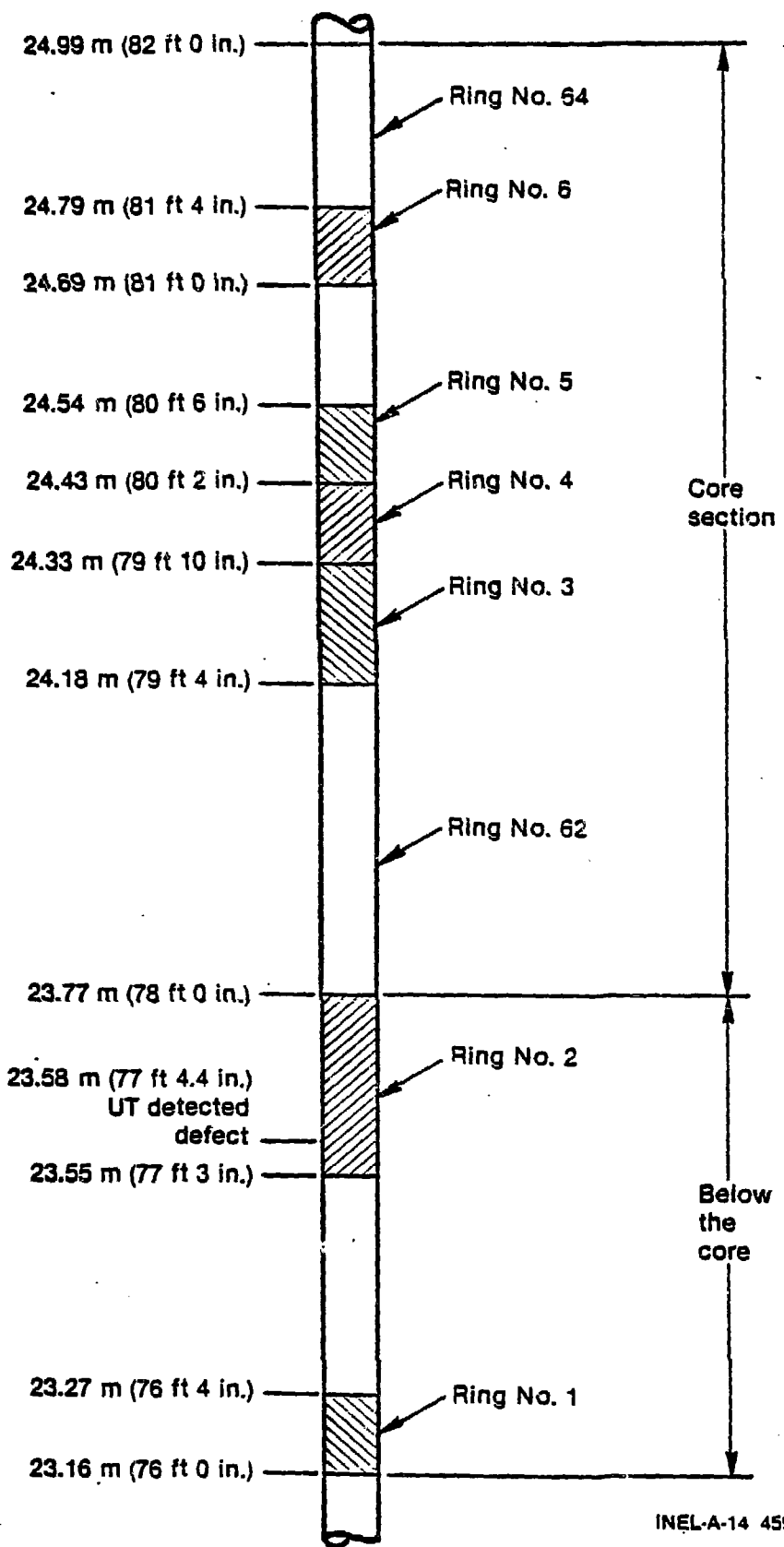


Figure 1. Location of test sections and rings.

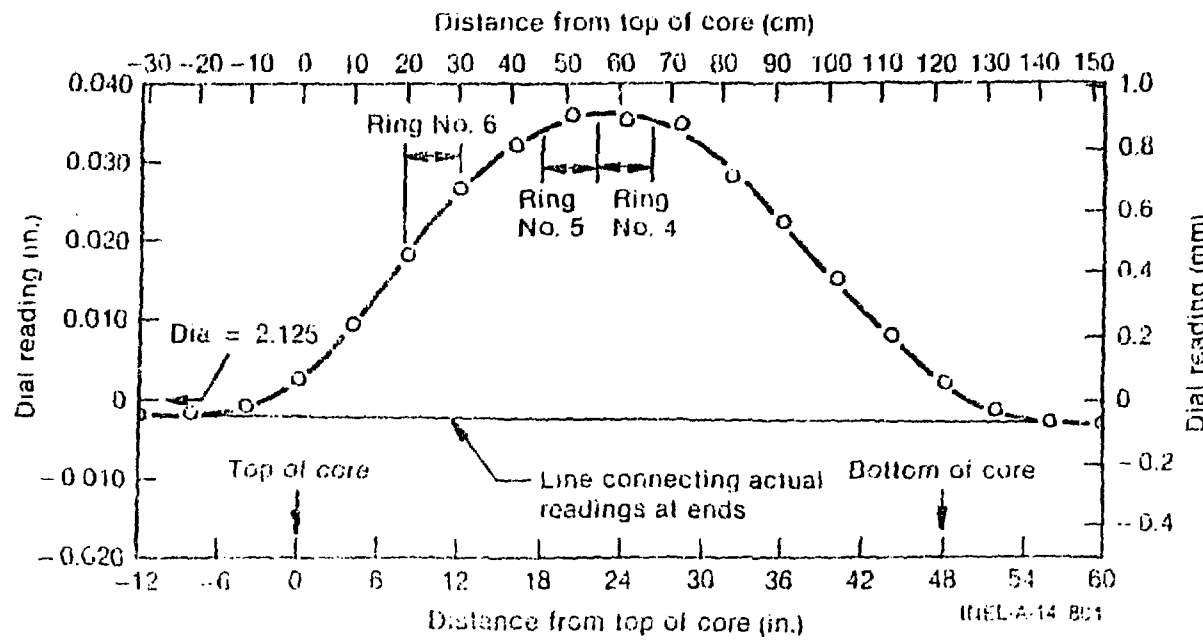


Figure 2. Bore gage measurements.

maximum  $\Delta D$  of 0.965 mm (0.038 in.) corresponding to a creep ( $\Delta D/D$ ) of 1.79 percent at the reactor centerline.

Measurements of the diameters and wall thickness of the six rings were in good agreement with the bore gage measurement and the design nominal dimensions. The average diameter change ( $\Delta D$ ) at ring 4 (core center) was 0.94 mm (0.037 in.), corresponding to a creep  $\Delta D/D$  of 1.74 percent. The nominal dimensions were OD - 6.43 cm (2.530 in.), ID - 5.40 cm (2.125 in.) and wall thickness - 0.51 cm (0.2025 in.).

## 2.2 Straightness Measurements

The straightness was measured to compare with bowing calculated from the swelling equation  $\Delta V/V$ <sup>[6]</sup> and from the relationship of the swelling to a pseudo-thermal behavior. The straightness of the 1.2 m (4 ft) core section of the in-pile tube was measured on fixed centers attached to an optical bench. Measurements were made at 5 cm length

intervals every 45 degrees around the periphery of the section with a dial gage which traveled on the optical bench. These measurements consisted of the distance from the reference to the outer diameter surface of the tube. Plots were made of these measurements and the maximum deviations from a straight line connecting the 1.2 m (4 ft) long section ends are given in Figure 3 with the degree indication. The bulge is calculated by combining algebraically the two deviations 180 degrees apart. The bow is calculated as the average of the algebraic difference between these deviations (difference divided by two) and is thus the shift of the center along a plane of the section. The maximum bulge and bowing are given in Figure 3. The maximum bow is 0.508 mm (0.020 in.).

The bowing was calculated<sup>[7]</sup> by the finite-element structural computer model SAP using the swelling equation adjusted from the Nuclear Systems Materials Handbook<sup>[8]</sup> as:

$$\frac{\Delta V}{V} = R \left[ \rho_f + \frac{1}{\beta} \left\{ \ln \frac{1 - \exp \beta_f \tau - \Phi_f}{1 + \exp \beta_f \tau} \right\} \right] \quad (1)$$

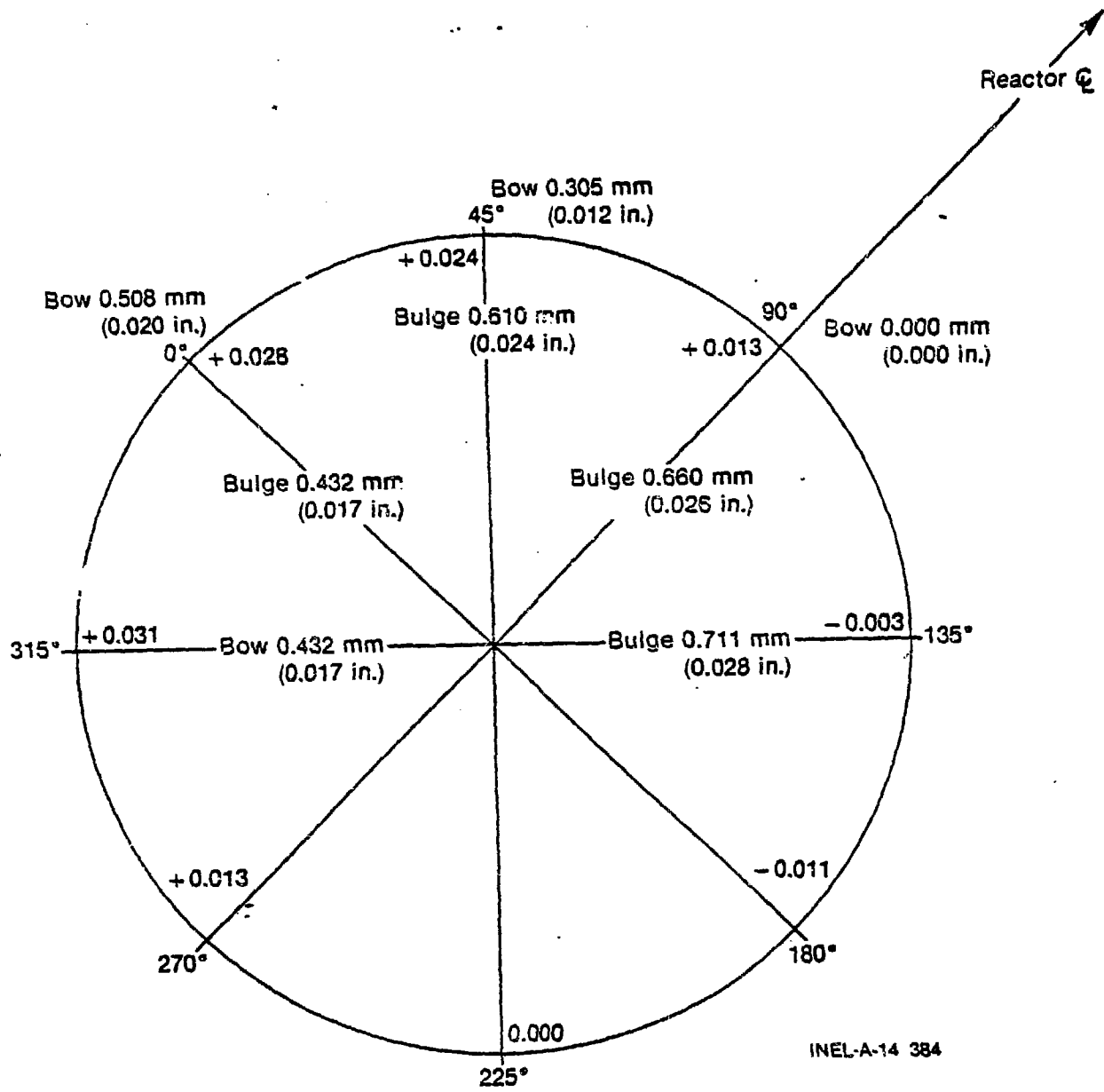


Figure 3. Bulge and bow in four-foot section.

where

$$R = 0.01 \exp[-49.77 + 0.196T - (1.87 \times 10^{-4})T^2],$$

$$\beta = -1.2 + (6.9 \times 10^{-3})T,$$

$$\tau = (7.99 - (2.98 \times 10^{-2})T + (2.9 \times 10^{-5})T^2)^{-1},$$

$\Phi t$  = fluence in units of  $10^{22}$  n/cm<sup>2</sup>  $E > 0.1$  MeV,

and

T = temperature in degrees Celsius.

The swelling was converted to a pseudo-thermal temperature across the tube (hot stripe to cold stripe) from the equation

$$\Delta T = \frac{\epsilon_0(F) - \epsilon_1(F)}{\alpha} = \frac{1}{3} \frac{(\Delta V/V)_0 - (\Delta V/V)_1}{\alpha} \quad (2)$$

where

$(F)$  = elongation as a function of fluence on the  
hot stripe and cold stripe of the wall, and

$\alpha$  = thermal expansion coefficient in inverse  
Celsius degrees.

From the pseudo-thermal expansion a bending stress  
 $\sigma_b$  results corresponding to the bowing of the tube  
as

$$\sigma_b = \frac{M_c}{I} \quad (3)$$

where

$M$  = bending moment

$C$  = distance of outer fibers to the neutral axis,  
and

$I$  = moment of inertia.

The bending stress is about 20.7 MPa (3 ksi) and the bowing 0.56 mm (0.022 in.). Thus, the calculated bowing from this model agrees with the measured bowing.

### 2.3 Specimen Preparation and Fluence Determination

Specimens were cut from the rings with a milling machine in the hot cells. The dimensions and orientation of the tensile and fracture toughness specimens with respect to the rings are given in Figure 4. The fast neutron fluence ( $E > 1$  MeV) of the ATR In-Pile Tube (IPT) SN-5 was measured from metal chips produced in machining the specimens. The metal chips were collected between specimen blanks. The fast neutron fluence was determined from the amount of  $^{54}\text{Mn}$  produced by the  $^{54}\text{Fe}(n,p)$   $^{54}\text{Mn}$  reaction. (This is a threshold reaction responding to neutrons with energies between  $\sim 2.5$  and 7.8 MeV.) The neutron fluence is reported as  $E > 1$  MeV based on a fission-spectrum-averaged cross section of 77.7 mb<sup>[9]</sup> and assuming that 69.2% of the neutrons have energies above 1 MeV. The fluence

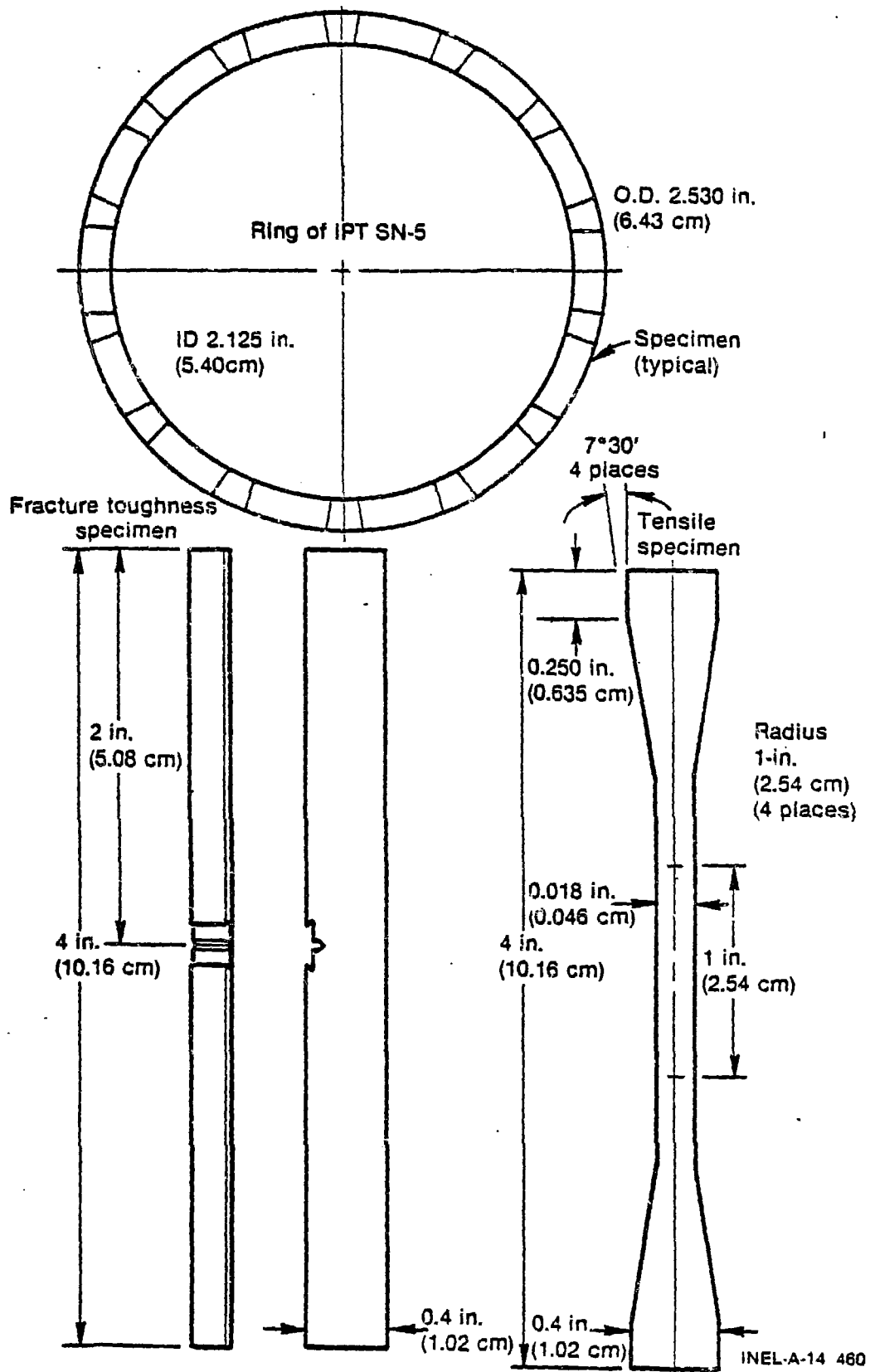


Figure 4. Test specimen configuration and orientation.

above 0.1 MeV energy can be estimated by multiplying by 1.92. The equivalent-damage-fluence to that of a fast reactor spectrum can be estimated by multiplying by a factor of three (3). For example, the ratio of the displacement cross section,  $\bar{D}$ , for stainless steel in an ATR core spectrum position with energies  $E > 0.1$  MeV to that of stainless steel data in the Nuclear Systems Materials Handbook for a fast reactor spectrum was found<sup>[10]</sup> to be  $1.6 \pm 0.2$ ; thus the equivalent damage-fluence for the ATR fluence  $E > 1$  Mev would be obtained by multiplying by the factor  $(1.6 \times 1.92) \approx 3$ .

### 3. RESULTS

#### 3.1 Immersion Density

The immersion density of slices (blanks) from the tube sections was measured per ASTM E 453, using water with Photoflow as a wetting agent. The data are given in Table 1. The nominal density value of  $7.9360 \text{ g/cm}^3$  for the unirradiated material was the same as used for an Engineering Test Reactor tube H-10. [11] The average volume change of 0.19 percent at an average fluence of  $2.63 \times 10^{22} \text{ n/cm}^2$  corresponds to an H-10 material average volume change of 0.21 percent at an average fluence of  $3.23 \times 10^{22} \text{ n/cm}^2$ .

#### 3.2 Irradiation Creep

Irradiation creep strain is obtained by assuming the relationship<sup>[4]</sup>  $\% \epsilon_{\text{irrad.creep}} = \% \epsilon_{\text{total}} + \% \epsilon_{\text{densification}} - \% \epsilon_{\text{swelling}} - \% \epsilon_{\text{thermal}}$ .

TABLE 1. DENSITY OF BLANKS FROM SN-5 TUBE

Sample No.	Fluence n/cm x 10 <sup>-22</sup> (E>1MeV)	Irradiated Density g/cm <sup>3</sup>	Density* Change g/cm <sup>3</sup>	Volume Change ΔV/V (%)
9	0.0002	7.9296	0.0064	0.08
20	0.0002	7.9249	0.0111	0.14
31	1.84	7.9222	0.0138	0.17
39	2.81	7.9196	0.0164	0.21
41	2.66	7.9210	0.0150	0.19
42	2.60	7.9211	0.0149	0.19
43	2.57	7.9210	0.0150	0.19
44	2.55	7.9213	0.0147	0.19

\*Density change from unirradiated value of 7.9360  
g/cm<sup>3</sup>.

The densification calculated according to the correlation for Type 316 stainless steel of Garner, Bates, and Gilbert<sup>[12]</sup> is small ( $\Delta\rho/\rho_0 = 0.05\%$ ). Thermal creep of an ATR irradiated pressure tube for a steady-state temperature gradient of 602 to 696 K (624 to 793°F) and 40 transient cycles (3.3 years) was zero<sup>[13]</sup>. Thus the maximum irradiation creep is approximately equal to the total creep, since

$$\% \epsilon_{\text{irrad.creep}} = 1.79 \% + 0.05/3\% - 0.19/3\% - 0.00\% = 1.71\%.$$

For the ETR data<sup>[11]</sup> the irradiation creep may be calculated from the equation [3,6]:

$$\frac{\epsilon_i}{\sigma} = C\phi t + D\frac{\Delta V}{V} \quad (4)$$

where

$\epsilon_i$  = irradiation creep

$\sigma$  = hoop stress (psi)

$\phi t$  = equivalent fluence in units of  $10^{22} \text{n/cm}^2$ ,  
 $E > 0.1 \text{ MeV}$ , and

$\Delta V/V$  = fractional swelling.

Slit width tests were made and reported<sup>[14]</sup> in which differential swelling stresses and thermal stresses undergo relaxation at temperatures less than 700 K due to irradiation creep. Stress relaxation allows for increased tube service life as compared with no stress relaxation. A comparison of density, swelling, and creep of ETR H-10 and ATR SN-5 tube material is given in Table 2.

### 3.3 Tensile Tests

The tensile tests were made on an Instron machine at a cross head speed of 0.05 ipm. The axial orientation and the shape of the tensile specimens cut from rings of the SN-5 IPT, were indicated in Figure 4. Grips were made to fit the tapered specimen's head so that failure would occur in the gage section. The tensile test data are given in Table 3. As a basis for comparing the tensile test results with other data and determining whether the irradiation creep has been damaging, the tensile results from ETR H-10<sup>[11]</sup> are given in Table 4. These results and average values at each test

TABLE 2. COMPARISON OF DENSITY, SWELLING, AND CREEP OF ETR H-10 AND ATR SN-5 MATERIAL

<u>Position</u>	<u>Average Fluence <math>\times 10^{-22} \text{ n/cm}^2</math> <math>E &gt; 1 \text{ MeV}</math></u>	<u>Density <math>\text{g/cm}^3</math></u>	<u>Swelling <math>\frac{\Delta V}{V}</math></u>	<u>Diameter Change <math>\Delta D</math></u>	<u>Irradiation Creep <math>\epsilon_i</math> %</u>
Base	0	7.9360	--	--	--
ETR (three specimens)	3.23(ave)	7.9182(ave)	0.0022(ave)	0.018	0.85
ATR-1	0.0002	7.929	0.0009	0.000	0.00
ATR-4 (five specimens)	2.64(ave)	7.9208(ave)	0.0019(ave)	0.038	1.79
ATR-5	2.50	--	0.0018(est)	0.036	1.69
ATR-6	1.97	7.9222	0.0017	0.024	1.13

TABLE 3. ATR SN-5 IPT TENSILE TEST DATA

Specimen No.	Fluence E>1MeV x10 <sup>-22</sup> n/cm <sup>2</sup>	In-reactor Creep %	Test Temperature K	Yield Strength σ <sub>ys</sub> MPa	Ultimate Tensile Strength σ <sub>uts</sub> MPa	Uniform Elongation in 2.54 cm %	Total* Elongation in 2.54 cm %	Total Specimen Elongation in 4.6 cm %	Estimated Modulus GPa
11	0.0002	0.0	297	388.8	654.9	>15	47	49	--
12	0.0002	0.0	297	394.3	689.4	>15	70	66	--
19	2.45	1.7	297	1036.2	1191.3	2.0	2.4	7	195.1
32	1.90	1.1	297	1074.9	1143.7	1.8	2.2	7	189.6
33	1.93	1.1	297	1062.4	1127.2	1.8	2.0	7	202.7
45	2.49	1.8	297	1065.1	1185.0	1.5	1.8	10	193.7
46	2.50	1.8	297	1098.2	1179.6	1.7	1.9	11	195.8
20	2.42	1.7	700	861.8	872.1	1.2	1.4	3	134.4
34	1.95	1.1	700	900.4	906.6	1.0	1.2	5	136.5
35	1.97	1.1	700	812.1	819.0	1.1	1.3	7	134.4
47	2.55	1.8	700	818.3	823.1	1.1	1.3	5	130.3
48	2.59	1.8	700	834.2	840.4	1.0	1.2	6	147.5
21	2.35	1.7	811	555.7	555.7	0.6	0.6	4	110.3
36	1.99	1.1	811	583.9	590.1	1.2	1.5	2	90.3
37	2.02	1.1	811	583.9	597.7	1.2	1.3	2	106.2
49	2.65	1.8	811	552.9	552.9	0.6	0.6	1	--
50	2.70	1.8	811	539.8	539.8	0.7	1.4	4	102.0
22	2.30	1.7	1061	172.4	172.4	0.0	0.3	2	--
23	2.24	1.7	1061	153.7	157.2	0.7	0.8	1	72.4
24	2.22	1.7	1061	250.9	255.8	0.7	0.8	3	87.6

\* Total elongation to rapid fall off in load except for specimens 11 and 12 which were measured on 2.54 cm specimen gage marks. Most specimens failed close to the extensometer knife edge.

TABLE 4. H-10 TENSILE TEST DATA AS FUNCTION OF TEST TEMPERATURE<sup>[11]</sup>

Number of Specimens	Average Fluence $n/cm^2 \times 10^{-22}$	In-reactor Creep %	Test Temperature K	Yield Strength MPa	Ultimate Strength MPa	Uniform Elongation % in 2.54 cm
5	$2.75 \pm 0.74$	0.66	297	$970.7 \pm 13.1$	$1007.2 \pm 13.8$	$1.52 \pm 0.11$
3	$3.09 \pm 0.46$	0.74	589	$845.9 \pm 17.9$	$850.0 \pm 16.5$	$0.90 \pm 0.29$
4	$2.96 \pm 0.69$	0.71	700	$759.7 \pm 11.7$	$763.2 \pm 13.1$	$0.80 \pm 0.11$
3	$2.66 \pm 0.79$	0.64	811	$595.0 \pm 31.0$	$609.4 \pm 25.5$	$1.02 \pm 0.12$

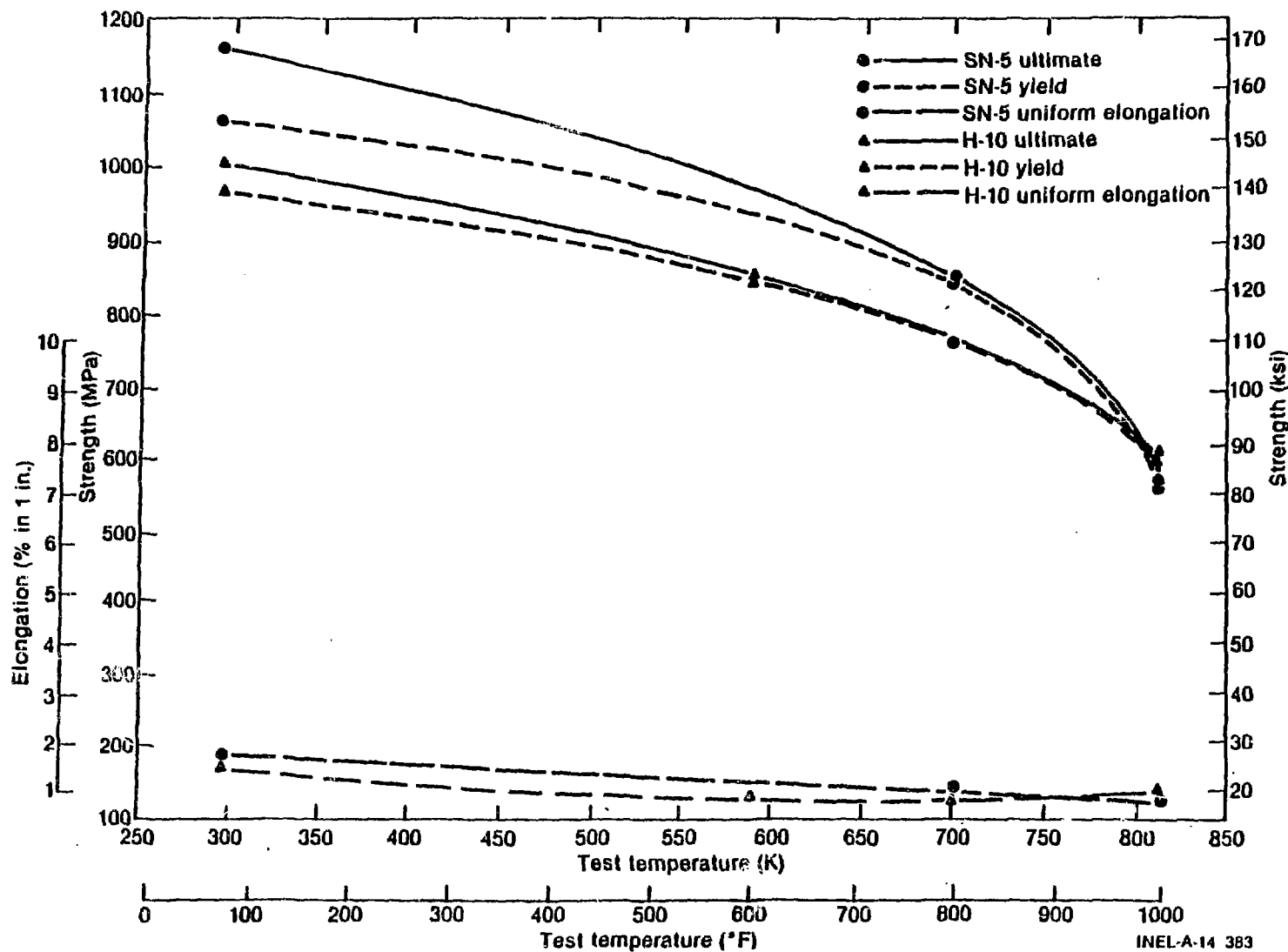


Figure 5. Comparison of tensile properties of ATR SN-5 and ETR H-10 material.

temperature from Table 3 are plotted in Figure 5. The comparison indicates a higher yield and ultimate strength in the SN-5 data with higher irradiation creep. However, a lower uniform elongation, and hence a lower toughness does not correspond to the higher strength. In fact inspection of the data of Table 3 at each test temperature does not indicate a consistent effect of irradiation creep on the strength or ductility. Hence there appears to be no damaging effect of irradiation creep on the tensile properties.

### 3.4 Fracture Toughness Tests

The fracture toughness tests were conducted by Bettis Atomic Power Laboratory (BAPL) on specimens as indicated in Figure 4. The single-edge-notched specimens were fatigue precracked and tested following ASTM E-399. Specimen thickness B was limited by tube wall thickness, but as fracture toughness goes down and tensile yield strength goes up, the tests should converge to a valid fracture toughness determination. The data for the ATR SN-5 tests are given in Table 5, and for ETR H-10 tests [11]

TABLE 5. SN-5 FRACTURE TOUGHNESS VALUES

Specimen No.	Test Temperature K	Fluence $E > 1 \text{ MeV}$ $\times 10^{-22} \text{ n/cm}^2$	Fracture Toughness $K_Q$ (MPa $\text{m}^{1/2}$ )	Maximum Load $P_{\text{max}}$ (newton)	5% Secant Load $P_Q$ (newton)	Ratio $P_{\text{max}}/P_Q$	Ratio $a/w$	Notched to Yield Strength Ratio $R_s$	In-reactor Creep %
26	297	2.06	61.4	14,100	10,564	1.33	0.47	0.48	1.1
41	297	2.70	62.7	12,210	9,786	1.25	0.498	0.44	1.8
28	297	2.00	68.4	13,700	11,565	1.18	0.48	0.48	1.1
39	297	2.80	72.8	16,057	14,456	1.11	0.415	0.50	1.8
29	700	1.90	72.7	15,390	13,566	1.13	0.465	0.66	1.1
43	700	2.58	51.2	13,144	12,454	1.06	0.415	0.51	1.8
44	700	2.50	54.9	10,030	7,784	1.29	0.509	0.51	1.8
30	700	1.84	61.9	12,388	8,229	1.51	0.52	0.59	1.1
42	700	2.60	49.7	9,897	7,339	1.35	0.48	0.44	1.8
31	700	1.87	63.5	11,921	9,563	1.25	0.50	0.55	1.1
27	700	2.06	59.4	10,520	6,894	1.53	0.54	0.53	1.1
9	700	0.0002	27.2	9,408	4,226	2.23	0.54	-	0.0
10	297	0.0002	82.3	12,966	5,560	2.33	0.53	1.36	0.0

are given in Table 6. The data plotted in Figure 6 are represented by four equations, and an extension is made of the data at 700 K (800°F) at the higher tensile yield and lower fracture toughness values.

Least squares regression analysis of the thirteen ETR H-10 data points gives:

$$K_Q = 120 - 8.08 (\phi t) \text{ with } \sigma = 14.1 \text{ MPa m}^{1/2} \quad (5)$$

Least squares regression analysis of the eleven ATR SN-5 data points gives:

$$K_Q = 75.9 - 6.30 (\phi t) \text{ with } \sigma = 7.78 \text{ MPa m}^{1/2} \quad (6)$$

In both equations  $\phi t$  is in units of  $10^{22} \text{ n/cm}^2$  ( $E > 1 \text{ MeV}$ ). A damaging effect which lowers the fracture toughness appears to be present in the ATR data equation (6).

The significance of the test temperature in the Figure 6 data is that a lower fracture toughness occurs at test temperature of 700 K than occurs for

TABLE 6. ETR II-10 FRACTURE TOUGHNESS DATA<sup>[11]</sup>

Specimen No.	Fluence E > 1 MeV x 10 <sup>-22</sup> n/cm <sup>2</sup>	Test Temperature K	Fracture Toughness K <sub>0</sub> MPa m <sup>1/2</sup>	Load Maximum P <sub>max</sub> newton	Load 5% Secant P <sub>0</sub> newton	Ratio P <sub>max</sub> / P <sub>0</sub>	Ratio a / w	Notched to Yield Strength Ratio R <sub>s</sub>	In-reactor Creep %
HD 2	3.48	297	107.3	44,480	33,360	1.33	0.25	0.95	0.84
HD 3	3.48	297	82.0	7,228	6,227	1.16	0.67	0.35	0.84
IID 4	3.48	297	99.0	19,126	16,013	1.19	0.50	0.61	0.84
IIG 2	2.58	297	107.6	30,380	26,021	1.17	0.40	0.81	0.62
IIA 2	1.93	297	90.0	12,454	11,565	1.08	0.55	0.44	0.46
HD 1	3.40	589	89.9	28,334	24,464	1.16	0.36	0.81	0.84
IIG 3	2.58	589	88.1	28,022	23,130	1.21	0.37	0.82	0.62
HD 6	3.48	700	73.0	26,688	20,016	1.33	0.36	0.85	0.84
IIG 4	2.58	700	82.4	24,953	20,683	1.21	0.39	0.84	0.62
HE 6	3.19	700	102.4	29,490	26,688	1.11	0.37	0.96	0.77
HD 5	3.48	700	100.8	>28,467	22,240	1.28	0.43	1.02	0.84
IIA 4	1.93	700	128.9	23,752	18,237	1.30	0.52	1.01	0.46
IIA 5	1.93	700	103.6	16,547	16,458	1.01	0.50	0.68	0.46

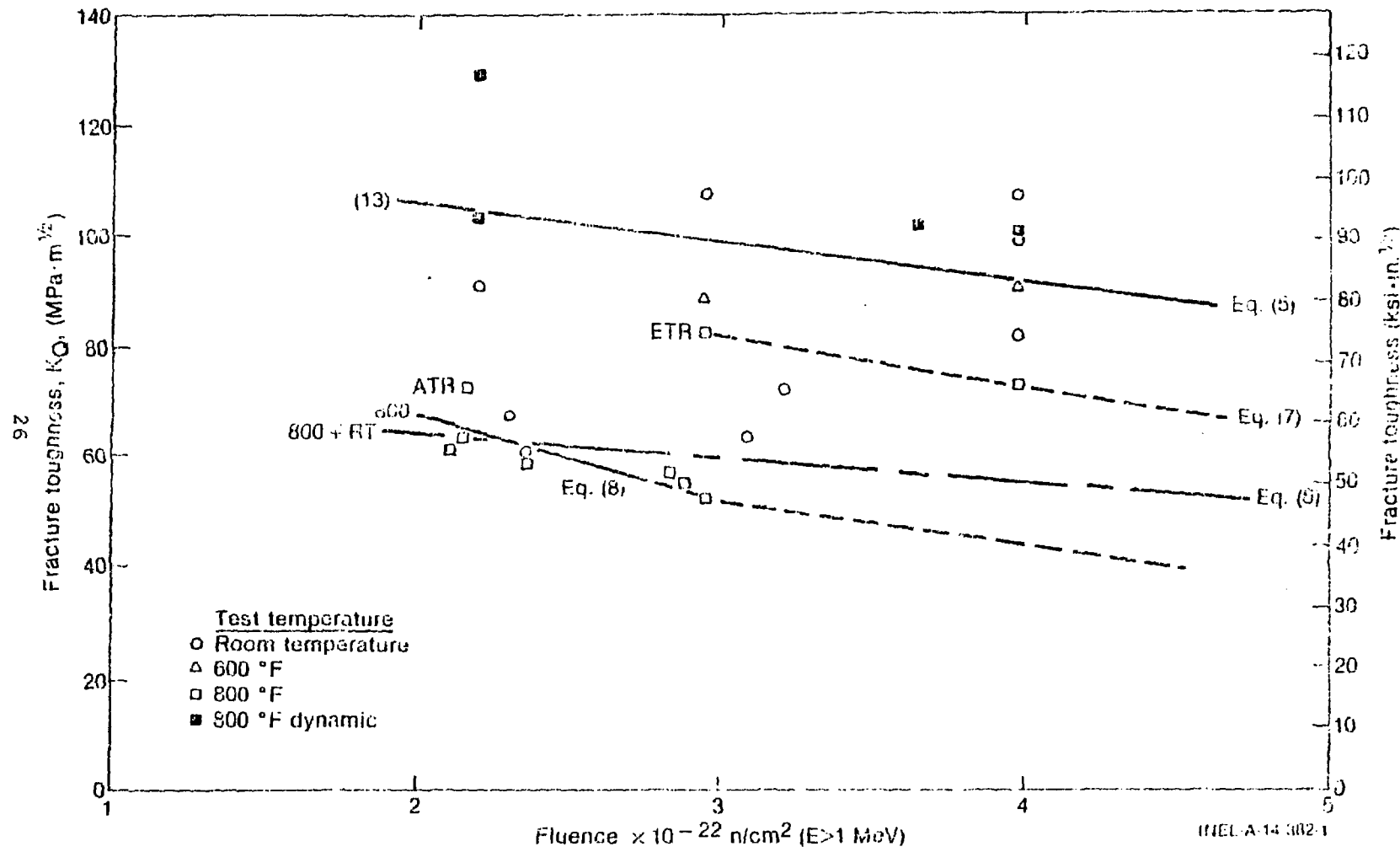


Figure 6. Fracture toughness of ATR SN-5 and ETR H-10 specimens.

linear regression analysis of data at all test temperatures. For ETR at 700 K,  $K_Q = 109.3 - 10.4(\phi t)$  (7); for ATR at 700 K,  $K_Q = 102.2 - 19.7(\phi t)$  (8) with  $\sigma = 4.32 \text{ MPa m}^{1/2}$ .

The significance of irradiation creep in reducing the fracture toughness is examined by evaluation of the fracture toughness as a function of irradiation creep. A least squares regression analysis of the ETR and ATR test points at 700 K gives:  $K_Q = 123.2 - 43.3(\epsilon_i \%)$  (9) with a correlation coefficient of 0.84. A high correlation coefficient is indicative that the fracture toughness is a function of the independent variable, i.e., irradiation creep. The regression model for irradiation creep was examined for fit of the data by an analysis of variance which indicated a significant F test of 26.5 with 12 degrees of freedom. The model had a multiple correlation coefficient of 0.71, which further indicates that the data fit the model.

The specimen notch strength to yield strength ratio,  $R_s$ , is a useful comparative measure of the

toughness of materials when the specimens are of the same form and size, and the size is insufficient to provide a valid  $K_{Ic}$  determination. The maximum load should result after pronounced crack extension prior to plastic instability and is therefore not the basis for a valid  $K_{Ic}$  determination. The gage dimension of the ETR specimen was 0.2 x 0.4. The notch-to-width ratio for both ETR and ATR specimens was 0.25, with an average a/w ratio at test of 0.44 for ETR and 0.48 for ATR. These sizes are so close that it is considered significant that the notch to yield strength ratio for the ETR specimens is 0.78 while that of the ATR are only 0.51. Thus, the notch strength to yield strength ratio ( $R_s$ ) indicates the ATR material is slightly less tough as was also indicated by the fracture toughness tests.

Extension of the ATR line (Equation 8) to higher fluence would include an increased damaging effect of irradiation creep as indicated by Equation 9 and is not justified for tubes which would have irradiation creep values  $\leq$  1.7 percent.

If a point of inflection is taken in the ATR line (Equation 8) at an irradiation creep value of 1.7 percent, the fracture toughness by Equation 9 at the point of inflection would be  $49.6 \text{ MPa m}^{1/2}$  (45.1 ksi in. $^{1/2}$ ). The dashed extension of the ATR line was made with the same slope as the equation 5 curve.

### 3.5 Creep-rupture Tests

Stress-rupture tests are basically creep tests carried to specimen failure but generally with higher loads. The aim here was to produce both creep and rupture data, hence creep-rupture tests. The specimens were similar to tensile specimens and were tested on an Instron machine at a nominal constant load. The machine set-up required varying the load from the set point  $\pm 20$  pounds on the load cell. In some tests the extensometer slipped so that minimum creep rates and elongation in 2.54 cm (1 in.) gage length of the extensometer was not obtained. The data are given in Table 7, and plotted in Figure 7.

TABLE 7. CREEP-RUPTURE TEST DATA FROM SN-5

Specimen No.	Test Temperature K	Fluence $E > 1 \text{ MeV}$ $\times 10^{-22} \text{ n/cm}^2$	Load newton	Stress MPa	Minimum Creep Rate $\times 10^6 \text{ (hr}^{-1}\text{)}$	Rupture Time	Elongation % in 2.54 cm
13	700	3.03	7,784	333.0	--	>304	--
	700		9,519	407.4	--	--	--
	700		10,230	437.8	--	18	0.26
14	700	3.17	9,563	409.5	1.8	258	0.10
15	700	3.14	9,341	399.9	3.1	61	0.11
16	700	3.03	9,074	393.0	3.3	43	0.05
52	700	3.20	8,362	355.7	1.3	419	0.06
17	811	3.01	4,448	191.7	1.2	1593+	0.37+
			5,338	229.6	4.9	56	--
18	811	2.91	8,562	364.7	--	0.2	--
56	811	2.80	9,563	407.4	--	0.4	--
55	811	2.34	6,494	290.9	--	0.5	--
51	811	3.14	4,982	211.0	2.3	2100	0.52

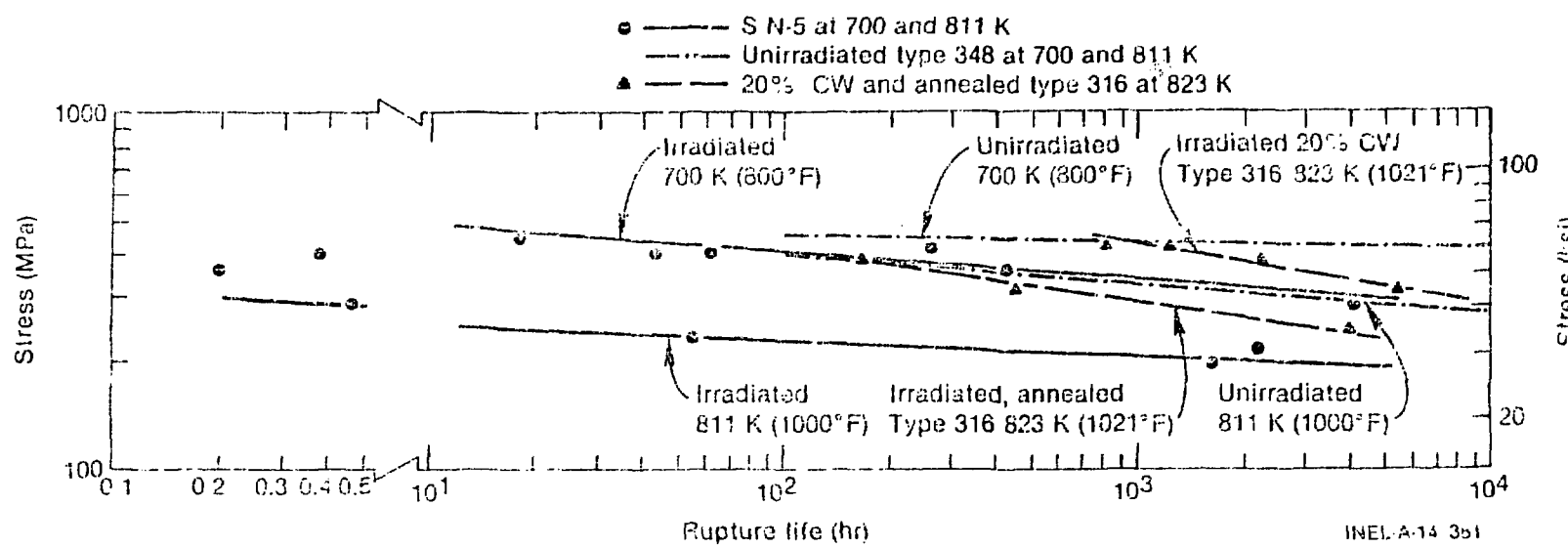


Figure 7. Rupture stress and life of irradiated SN-5, unirradiated Type 348, and Type 316 irradiated stainless steel.

The delayed-failure stress-rupture test on ETR H-10 material was made at 811 K on an unnotched specimen, which failed upon loading at a stress of 543.9 MPa. This is a much higher failure stress than the 811 K (1000 F) values for the ATR specimens reported in Table 7. Comparison is difficult because of the limited data. However, examination of Figure 7 indicates that the creep-rupture strengths of the ATR SN-5 Type 348 stainless steel specimens at 700 K and 811 K are lower than for unirradiated Type 348 at these temperatures<sup>[15]</sup>, and also lower than for irradiated cold-worked or annealed Type 316 stainless steel<sup>[16]</sup>.

#### 4. DISCUSSION

The maximum observed swelling ( $\Delta V/V$ ) for the ATR SN-5 material appears consistent both with the measured bowing and with swelling calculated by Equation 1 for an operating temperature of 629 K. The irradiation creep, however, is greater than that calculated by Equation 4. For example, using Equation 4 constants which have been adjusted for the ETR data, the SN-5 measured swelling of 0.0019, the hoop stress of 11,500 psi, and an equivalent fluence of 7.92 (fluence in units of  $10^{22} \text{ n/cm}^2 \text{ E} > 1 \text{ MeV}$  multiplied by 3 to account for spectrum and displacement cross section) the value of the irradiation creep obtained is:

$$\epsilon_i = 11,500 (5.88 \times 10^{-8} \times 7.92 + 1.5 \times 10^{-5} \times 0.0019) = 0.0057.$$

Thus, the measured irradiation creep of 1.71% is three times greater than calculated by Equation 4 even though Equation 4 has been adjusted to give a higher irradiation creep than fast reactor data<sup>[6]</sup> at equivalent damage fluence.

This additional irradiation creep is believed to be responsible for the damaging effect on the fracture toughness of the SN-5 material in post irradiation tests as compared with the H-10 material. It was shown that a relationship (Equation 9) existed between the ETR and ATR test data at 700 K for the fracture toughness with irradiation creep as the independent variable. The fracture toughness measured in the postirradiation tests should be conservative for in-reactor conditions since as pointed out by Bloom and Wolfer<sup>[5]</sup> the in-reactor rupture life was longer than predicted by post-irradiation tests. The apparent cause was retardation of the initiation or growth of cracks during irradiation creep as a result of stress relaxation at the crack tip.

The average tensile test ductility (uniform elongation) in both 700 K and room temperature tests was greater for the SN-5 material than for the H-10 material, even though the SN-5 yield and ultimate strengths were greater. The tensile ductility behavior seems to agree with the post-irradiation

biaxial stress rupture tests of Duncan<sup>[4]</sup> although the irradiation creep was greater for the tensile tests (1.8 percent versus 1 percent). For fracture toughness tests with lower irradiation creep values (> 1.0 percent) a discernible effect of irradiation creep is present only in the relationship for fracture toughness versus irradiation creep (Equation 9).

A relationship between tensile properties, microstructure, and fracture toughness is expected<sup>[17]</sup>. Qualitatively increased yield strength and decreased fracture strain accompany decreased fracture toughness. The trend of decreasing fracture toughness with increasing yield strength is related to both microstructure and crack tip instability. In the preliminary investigation of the microstructure, the TEM photographs did not reveal differences from the H-10 tube material which could be related to crack tip instability to explain the decrease in fracture toughness.

## 5. SUMMARY

The irradiation creep of 1.0 to 1.7 percent in the ATR SN-5 Type 348 material has been damaging to the fracture toughness as compared with irradiated ETR H-10 Type 348 stainless steel with irradiation creep of 0.4 to 0.9 percent. The creep-rupture strength also seems to be reduced.

The post-irradiation properties of the Type 348 stainless steel tube may be summarized as follows:

1. The bowing across a 1.8 m tube section was 0.51 mm and can be calculated from swelling equations.
2. The average volume change ( $\Delta V/V$ ) was measured by immersion density to be 0.19 percent at a fluence of  $2.63 \times 10^{22} \text{ n/cm}^2$  ( $E > 1 \text{ MeV}$ ).

3. The tensile yield and ultimate strength were 845.2 and 852.1 MPa, respectively, at 700 K and average fluence of  $2.29 \times 10^{22} \text{ n/cm}^2$  while the uniform elongation was 1.08 percent.
4. The fracture toughness at 700 K and fluence of  $2.56 \times 10^{22} \text{ n/cm}^2$  was  $51.8 \text{ MPa} \cdot \text{m}^{1/2}$  ( $47.1 \text{ ksi} \cdot \text{in.}^{1/2}$ ).
5. The creep rupture strength at 700 K for 1000 hours was about 331 MPa (48 ksi).

## 6. REFERENCES

- [1] Wolfer, W. G., "Formulation of Constitutive Laws for Deformation During Irradiation" in Effects of Radiation on Structural Materials, ASTM STP 683, 1979, pp. 581-597.
- [2] Wolfer, W. G., Ashkin, M., and Boltax, A., "Creep and Swelling Deformation in Structural Materials During Fast-Neutron Irradiation" in Properties of Reactor Structural Alloys After Neutron or Particle Irradiation, ASTM STP 570, 1975, pp. 233-258.
- [3] Boltax, A., Foster, J. P., Weiner, R. A., and Biancheria, A., "Void Swelling and Irradiation Creep Relationships" in Journal of Nuclear Materials, 65, 1977, pp. 174-183.
- [4] Duncan, D. R., "Effects of Irradiation Creep on Ex-Reactor Mechanical Properties" in Effects of Radiation on Structural Materials, ASTM STP 683, 1979, pp. 567-577.

[5] Bloom, E. E., and Wolfer, W. G., "In-reactor Deformation and Fracture of Austenitic Stainless Steels" in Effects of Radiation on Structural Materials, ASTM 683, 1979, pp. 656-672.

[6] Beeston, J. M. and Burr, T. K., In-reactor Stress Relaxation of Type 348 Stainless Steel In-pile Tube, ASTM STP 676, 1979, pp. 155-170.

[7] Harris, B. L., EG&G Idaho, Inc., private communication, January 23, 1980.

[8] TID-26666, Nuclear Systems Materials Handbook, Vol. 1, Design Data Property Code 3304 (E-1), p. 1.0, Section 4; Section 5, Revision 2, 4-16-75 and 6-19-74.

[9] ENDF/B-IV Dosimetry File, ENDF-216, April 1975, p. 284.

[10] Doran, D. G., Westinghouse Hanford Company, private communication, September 18, 1975.

[11] Krupowicz, J. J., Evaluation of the Mechanical Properties of an Irradiated, Type 347 Stainless Steel, In-pile Tube with a Peak Fluence of  $4 \times 10^{22} \text{ n/cm}^2 (> 1 \text{ MeV})$ , WAPD-TM-1425, August 1979.

[12] Garner, F. A., Bates, J. F., and Gibert, E. R., "Anisotropic Densification of Reference Steel", HEDL-SA-1023, September 1975.

[13] Burr, T. K., EG&G Idaho, Inc., private communication, November 28, 1977.

[14] Beeston, J. M. and Burr, T. K., "Stress Relaxation Analysis and Irradiation Creep and Swelling in Pressure Tubes", presented at the 5th International Conference on Structural Mechanics in Reactor Technology, Berlin, Germany, August 13-17, 1979, accepted for publication in International Journal of Pressure Vessels and Piping.

[15] Simmons, W. F. and Cross, H. C., "The Elevated Temperature Properties of Stainless Steels", ASTM STP 124, 1952), p. 75.

[16] Bloom, E. E. and Stiegler, J. O., "Effect of Irradiation on the Microstructure and Creep-Rupture Properties of Type 316 Stainless Steel", ASTM STP 526 (1973) pp. 360-382.

[17] Sailers, R. H., "Relationship Between Tensile Properties and Microscopically Ductile Plane-Strain Fracture Toughness" ASTM STP 605, 1976, pp. 34-61.